

## On the fundamentals of the virtual source method

Valeri Korneev<sup>1</sup> and Andrey Bakulin<sup>2</sup>

### ABSTRACT

The virtual source method (VSM) has been proposed as a practical approach to reduce distortions of seismic images caused by shallow, heterogeneous overburden. VSM is demanding at the acquisition stage because it requires placing downhole geophones below the most complex part of the heterogeneous overburden. Where such acquisition is possible, however, it pays off later at the processing stage because it does not require knowledge of the velocity model above the downhole receivers. This paper demonstrates that VSM can be viewed as an application of the Kirchhoff-Helmholtz integral (KHI) with an experimentally measured Green's function. Direct measurement of the Green's function ensures the effectiveness of the method in highly heterogeneous subsurface conditions.

### INTRODUCTION

Complexity of the near surface or overburden is a major complication in seismic imaging. Quite often this complexity is limited to the upper part of the section, as in cases of heterogeneous near-surface, basalt, and salt layers. The ability of existing imaging methods to eliminate distortions of the heterogeneous overburden remains fundamentally limited because they cannot account for all propagation complications. Bakulin and Calvert (2004, 2006) have proposed the virtual source method (VSM), which can eliminate distortions caused by overburden of any complexity. VSM is based on placing downhole geophones below the most complex overburden and directly measuring these propagation distortions (Figure 1). Schuster (2005) provides a simple kinematic explanation of how VSM and other interferometric techniques can eliminate overburden distortions. This paper goes beyond kinematic considerations. First, we derive the basic equation of VSM from the Kirchhoff-Helmholtz integral (KHI) for arbitrarily heterogeneous acoustic media. Then we speculate as to why VSM works so well,

even though many of its theoretical assumptions are not satisfied in practice.

### THEORY

Here we show that VSM can be derived directly from the KHI using the reciprocity principle. Seismic inverse methods utilize the ability of KHI to image subsurface structures by treating them as locations of secondary sources (diffractors) excited by a set of primary sources. Although the conditions for applying the KHI are not entirely met in practice, satisfactory imaging results are often obtained for reasons that are discussed below.

### KHI for heterogeneous acoustic media

Consider an acoustic field  $u(x, y, z, t)$  excited by a source at a point  $M_0$ . Such a field satisfies the equation of motion,

$$\nabla^2 u - \frac{1}{v^2(x, y, z)} \frac{\partial^2 u}{\partial t^2} = -\delta(M - M_0)w(t), \quad (1)$$

where propagation velocity  $v(x, y, z)$  is an arbitrary function of spatial coordinates;  $w(t)$  is a causal source time function ( $w(t) = 0$ , and  $u(t) = 0$ , when  $t < 0$ ); and  $\delta(M)$ , where  $M = (x, y, z)$ , is a spatial delta function. In the frequency domain, equation 1 takes the form

$$\nabla^2 \tilde{u} + \frac{\omega^2}{v^2(x, y, z)} \tilde{u} = -\delta(M - M_0)\tilde{w}(\omega), \quad (2)$$

where  $\tilde{u}(\omega)$  and  $\tilde{w}(\omega)$  are the Fourier transforms of the functions  $u$  and  $w$ , respectively, and  $\omega$  is radial frequency. If the field  $\tilde{u}$  (or  $u$ ) and its normal derivative are known everywhere on a closed surface  $\Sigma$  and volume  $V$ , then this field can be calculated at any internal point  $M$  of the volume  $V$  inside  $\Sigma$  (Morse and Feshbach, 1953):

$$\tilde{u}(M) = I_\Sigma(M) + I_V(M), \quad (3)$$

Manuscript received by the Editor August 24, 2005; revised manuscript received September 29, 2005; published online May 24, 2006.

<sup>1</sup>Lawrence Berkeley National Laboratory, 1 Cyclotron Road, Berkeley, California 94720. E-mail: vakorneev@lbl.gov.

<sup>2</sup>Shell International E&P Inc., 3737 Bellaire Boulevard, Houston, Texas 77025. E-mail: andrey.bakulin@shell.com.

© 2006 Society of Exploration Geophysicists. All rights reserved.

$$I_{\Sigma}(M) = \frac{1}{4\pi} \int_{\Sigma} \left( G(S, M) \frac{\partial \tilde{u}}{\partial n}(S) - \tilde{u}(S) \frac{\partial G(S, M)}{\partial n} \right) dS, \quad (3a)$$

$$I_V(M) = \tilde{w}(\omega) \int_V \delta(M - M_0) G(v, M) dv. \quad (3b)$$

Equation 3a represents the KHI, where integration is performed along the surface  $\Sigma$ , while in equation 3b integration goes over the volume  $V$ . Both equations 3a and 3b contain the causal Green's function  $G$ , which satisfies equation 2 when  $\tilde{w}(\omega) = 1$ . For outgoing fields, which are caused by sources located inside  $\Sigma$  and satisfy radiation conditions at infinity (Baker and Copson, 1950), the KHI does not contribute to  $\tilde{u}(M)$  since

$$I_{\Sigma}(M) = 0. \quad (4)$$

Therefore,  $\tilde{u}(M) = I_V(M) = \tilde{w}(\omega) G(M_0, M)$ , representing fields from the source located at point  $M_0$  inside volume  $V$ . In this case, the internal Green's function  $G(M_0, M)$  cannot be reconstructed formally from surface measurements of the fields  $\tilde{u}$  and  $\partial \tilde{u} / \partial n$  on  $\Sigma$ . In the next section, we prove that application of KHI to time-reversed fields allows such reconstruction. Other KHI derivations (Baker and Copson, 1950) isolate the source points by surrounding them with additional surfaces and substitute volume integrals of the type in equation 3b with the surface integrals of the type in equation 3a. Both approaches are equivalent.

The KHI is a mathematical expression of Huygens' principle, stating that the wavefield at any point can be reconstructed using radiation from secondary sources represented by displacements (monopoles) and displacement derivatives (dipoles) on the surface  $\Sigma$ . Equation 4 is a consequence of the Huygens-Fresnel principle for a case when both source and observation points are inside surface  $\Sigma$  and "the effect inside produced by the action of all secondary sources on  $\Sigma$  is however null" (Baker and Copson, 1950). The numerical application of KHI (equation 3a) is the basis for most

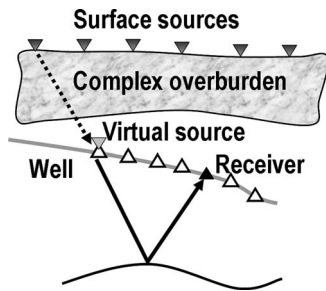


Figure 1. VSM is designed to image below complex overburden. Since surface shots are used in this example, it is essential to place borehole receivers in a well below the most distorting zone to directly measure the transmission response (Green's function). Time reversal is used to redatum surface shots into locations of downhole receivers without knowledge of the velocity model between them (Bakulin and Calvert, 2004, 2006). In redatumed downhole data, reflections from deeper targets are free from distortions caused by complex overburden. Therefore, conventional methods can be used to obtain high-fidelity seismic images from virtual source data.

seismic processing steps such as migration, tomography, and wavefield continuation. While Huygens' principle is usually illustrated for forward propagation, in all applications it is actually used for back propagation since we are interested in the wavefield at internal points.

### Derivation of the virtual source equation

Consider an array of identical sources  $D_i, (i = 1, 2, \dots, I)$  completely covering a surface  $\Sigma$  surrounding a heterogeneous volume  $V$ , with two buried receivers, A and B (Figure 2). Assume that at both A and B the values of the displacements  $\tilde{u}_{SA}, \tilde{u}_{SB}$  generated by (monopole) sources on  $\Sigma$  are known and that all sources emit the same amplitude  $\tilde{w}(\omega)$ . Also assume that the values of the derivatives  $\partial \tilde{u}_{SA} / \partial n, \partial \tilde{u}_{SB} / \partial n$  are known (these can be thought of as responses recorded when exciting dipole sources at the same surface locations). We demonstrate how to compute the response (seismogram) at B for the source at A from this data set without additional knowledge of the velocity structure between the surface shots and downhole receivers.

Fields  $\tilde{u}_{SA}(\omega)$  and  $\tilde{u}_{SB}(\omega)$  can be expressed as

$$\tilde{u}_{SA}(\omega) = \tilde{w}(\omega) G(S, A)$$

and

$$\tilde{u}_{SB}(\omega) = \tilde{w}(\omega) G(S, B) \quad (5)$$

using Green's functions  $G(S, A)$  and  $G(S, B)$ . Time-reversal operation for wavefields means a change of sign for time variable  $t$  and, correspondingly, a complex conjugation of spectra in the frequency domain. Time-reversed field  $G^*(M, A)$  therefore satisfies the equation

$$\nabla^2 G^*(M, A) + \frac{\omega^2}{v^2(x, y, z)} G^*(M, A) = -\delta(M - A), \quad (6)$$

which describes waves coming from infinity and collapsing on point A at  $t = 0$  (Petrashen and Nakhamkin, 1973). Equation 5 gives

$$G^*(S, A) = \tilde{u}_{SA}^*(\omega) / \tilde{w}^*(\omega) \quad (7)$$

for points S on surface  $\Sigma$ .

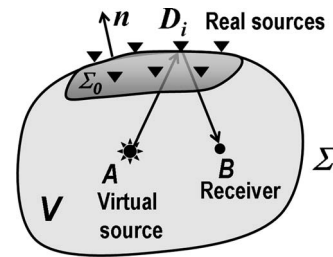


Figure 2. Generalized representation of the downhole seismic experiment used for the derivation. Volume  $V$  is surrounded by surface  $\Sigma$ . The sources may occupy either the entire surface (theory) or a portion of it ( $\Sigma_0$ ). Recording consists of two sets of measurements from each source to points A and B.

If we take the time-reversed Green's function  $G^*(M,A)$  as the wavefield  $u$  in equations 3, 3a, and 3b, then we obtain the following representation for  $G^*(A,B)$  in the form

$$G^*(A,B) = I_{\Sigma}(A,B) + G(A,B), \quad (8)$$

with the KHI given by

$$I_{\Sigma}(A,B) = \frac{1}{4\pi} \int_{\Sigma} \left( G(S,B) \frac{\partial G^*(S,A)}{\partial n} - G^*(S,A) \frac{\partial G(S,B)}{\partial n} \right) dS, \quad (9)$$

which is a function of points  $A$  and  $B$ . The second term in equation 8 is a result of volume integration as in equation 3. Note that the surface integral in equation 9 is nonzero because the time-reversed field  $G^*(S,A)$  represents ingoing waves and does not satisfy the radiation condition at infinity. Because of reciprocity,  $G^*(S,A) = G^*(A,S)$ , we need only to excite dipole and monopole sources at surface points  $S$  and record at points  $A$  and  $B$  in order to obtain the response

$$\begin{aligned} \tilde{U}(A,B) &= G(A,B) - G^*(A,B) \\ &= 2i \operatorname{Im} G(A,B) \\ &= -I_{\Sigma}(A,B), \end{aligned} \quad (10)$$

where field  $\tilde{U}(A,B)$  satisfies a homogeneous wave equation without a source term. From equation 10 we infer

$$\tilde{U}(A,B) = -\tilde{U}^*(A,B), \quad (11)$$

which means that corresponding to  $\tilde{U}(A,B)$ , the time-domain field  $U_{AB}(t)$  is antisymmetric:

$$U_{AB}(t) = -U_{AB}(-t). \quad (12)$$

Time-domain response  $g_{AB}(t)$  of the function  $G(A,B)$  is causal, which, together with equations 10 and 12, leads to

$$g_{AB}(t) = U_{AB}(t) = -U_{AB}(-t), \quad (t > 0). \quad (13)$$

From equation 13 it follows that the wave propagation process described by equation 10 consists of acausal ( $t < 0$ ) and causal ( $t > 0$ ) parts. Acausal propagation goes in reverse time until at  $t = 0$  it collapses into the virtual source at point  $A$ . Then, for  $t > 0$ , the propagation process starts again as if the source were fired at  $t = 0$  and the source wavelet sign were inverted (equation 10). Therefore, the field  $G(A,B)$  is generated by the back-propagating field  $G^*(A,B)$ . The sign inversion in equations 11 and 12 is a result of passing of the wavefield through a focal point  $A$  (Alexeev and Gelchinsky, 1958). Note that acausal and causal parts here carry the same information, so one of them is redundant if the other one is known. Therefore, the KHI in the form of equation 9 allows exact evaluation of the time-domain Green's function  $g_{AB}(t)$  between points  $A$  and  $B$ . This is illustrated on a synthetic data set by van

Manen et al. (2005). Wapenaar (2004) considers a similar problem when two points located at a free surface are illuminated by a set of unknown buried sources.

Combining equations 5 and 7–9, we also obtain

$$\begin{aligned} \tilde{U}(A,B) &= -\frac{1}{4\pi|\tilde{w}(\omega)|^2} \int_{\Sigma} \left( \tilde{u}(S,B) \frac{\partial \tilde{u}^*(S,A)}{\partial n} \right. \\ &\quad \left. - \tilde{u}^*(S,A) \frac{\partial \tilde{u}(S,B)}{\partial n} \right) dS, \end{aligned} \quad (14)$$

expressing response  $\tilde{U}(A,B)$  directly via wavefields recorded at points  $A$  and  $B$ .

Equation 14 is the fundamental result of KHI application resulting in VSM. It states that if the source amplitudes are known, then two sets of records between the closed surface  $\Sigma$  and two arbitrary points allow evaluation of the Green's function between these points as if one of them were the source and the other were the receiver. Both the KHI and the reciprocity principle used to derive formula 14 are rigorously proven and use no restrictions on complexity of the velocity function. When an actual recorded wavefield (equation 5) is used, then the computed response corresponds to the source at  $A$  emitting zero-phase amplitude  $|\tilde{w}(\omega)|^2$ . Such a symmetrical wavelet might violate the causality assumption around  $t = 0$  when points  $A$  and  $B$  are so close to each other that causal and acausal parts have some (small) overlap. Such overlap is expected to be insignificant in practical applications since it does not affect reflections from target horizons.

In the derivations above we assumed that fields in equation 5 result from recording times  $T$  that were long enough to ensure that all wave energy which passed surface  $\Sigma$  was recorded and that integration is performed over the whole  $\Sigma$ . In practice, however, it is never the case that all the functions on the right-hand side of equation 3 (or equation 14) are known. Instead, practical applications rely on simplifying assumptions and approximations, which are discussed in the next section.

## WHY THE KHI WORKS FOR SEISMIC DATA

Applications of the KHI for seismic data processing and imaging represents back propagation of the recorded (time-reversed) wavefields to image underground structures. These applications are compromised by three circumstances.

First, it is impossible, in principle, to record the field  $\tilde{u}$  over the entire closed surface  $\Sigma$ . In practice, we have only partial knowledge about the values of  $\tilde{u}$  on  $\Sigma$  over some localized area  $\Sigma_0$ , and fewer than several percent of the total aperture (volume angle) is covered by data. The rest of the field remains unknown and is artificially assumed to have zero values. The effects caused by limited apertures are thoroughly discussed by Petrashen and Nakhmkin (1973).

Second, measuring the spatial derivatives of the field  $\tilde{u}$  is difficult and is not done in practice. Moreover, the integrand in the KHI is nonzero only if neither the source nor the receiver points are located on the earth's free surface, which is realized only for cross-hole surveys. Indeed, if the field  $\tilde{u}$  represents pressure, then it (and the corresponding Green's function) has zero values on a free surface, and both integrand components in equation 3a are equal to zero. If  $\tilde{u}$  represents displacement, the normal derivatives in equa-

tion 3a are zero, reflecting the free-surface boundary conditions.

Finally, the evaluation of Green's function  $G$  requires detailed knowledge of the velocity function  $v(x, y, z)$ , which one never has. In fact, an essential purpose of seismic imaging is to obtain information about unknown rock parameters. Therefore, in processing algorithms, only simplified velocity models are used for approximate evaluations of  $G$ . An especially difficult problem in this respect is created by a highly heterogeneous and unknown overburden zone. The existence of such zones causes serious distortions in the traveling waves, even when the heterogeneity is located far from the target zone.

Despite these problems, a variety of seismic imaging algorithms based on the KHI perform reasonably well. This property can be understood better after expressing the recorded field  $\tilde{u}$  and the propagating field  $G$  in exponential form,

$$\tilde{u}^* = \tilde{u}_0 e^{-i\omega\tau_u}$$

and

$$G = G_0 e^{i\omega\tau_G}, \quad (15)$$

with spatially varying amplitude functions  $\tilde{u}_0$ ,  $G_0$ , and phase functions  $\tau_u$ ,  $\tau_G$ . The function  $\tau_G$  has the dimension of time and for homogeneous media is equal to the traveltimes of wave propagation between a point on  $\Sigma$  and a point  $B$  (Figure 2). Likewise, for homogeneous media,  $\tau_u$  describes the traveltimes between  $A$  and the integration point on the surface  $\Sigma$ . For complex heterogeneous media,  $\tau_u$  and  $\tau_G$  generally have no specific physical meaning and represent contributions from all possible propagating waves. Next, note that the normal derivatives of functions 15 are approximately proportional to these functions, but with slowly varying factors. This statement reflects the fact that wavefields and their derivatives propagate with the same wavefronts. For example, it is trivial to demonstrate that the corresponding phase shift between these two fields is equal to half a period for any plane wave. This explains why in conventional practice the imaging function has a general form

$$\tilde{u}(M) = \int_{\Sigma_0} W(S) G \tilde{u} dS = \int_{\Sigma_0} W(S) G_0 \tilde{u}_0 e^{i\omega(\tau_G - \tau_u)} dS, \quad (16)$$

which contains no spatial derivatives and is supplemented by a weighting function  $W(S)$ . If  $M = M_0$ , then ideally  $\tau_u = \tau_G$  and the integrand in equation 16 is a smoothly varying function describing constructive interference so that the integration results in a nonzero value. At other points, the integrand oscillates and the integration gives negligibly small values. For a sharp reconstructed image, it is critically important to eliminate oscillating factor  $e^{i\omega(\tau_G - \tau_u)}$  in equation 16. Although  $\tau_u$  is a measurement result and contains all propagating waves, the function  $\tau_G$  is only approximately known in most practical applications because it depends on the medium structure and the accuracy of the forward-modeling solver. Therefore, the accuracy of the estimation is the main factor that defines seismic image quality. The weighting factors  $W(S)$  (which usually describe geometrical spreading corrections) bring only second-order improvements. These conclusions are supported by a number

of analytical and numeric studies of KHI-based imaging algorithms (Vasil'yev, 1975; Timoshin, 1978).

The best possible way to evaluate the Green's function is through direct measurement. In this case the complexity of the medium becomes irrelevant. Time-reversal experiments (Fink and Prada, 2001) confirm that excellent focusing (via back-propagation) is possible even when late multiply scattered phases of the transmitted field are used. The key is to have reverse-time propagation in exactly the same medium in which forward propagation was recorded. Bakulin and Calvert (2004) use a similar concept in their VSM, which is an application of equation 16 with the Green's function taken directly from field measurements.

Indeed, let us assume that the wavefield from an array of sources  $D_i$ , ( $i = 1, 2, \dots, I$ ) is recorded at two points  $A$  and  $B$  (Figure 2) and the data include two sets of displacements  $u_{iA}(t)$ , ( $0 \leq t \leq T$ ) and  $u_{iB}(t)$ , ( $0 \leq t \leq T$ ) from all surface shots to receivers at  $A$  and  $B$ , respectively. In the frequency domain, the recorded data are given by

$$\tilde{u}_{iA}(\omega) = \tilde{w}(\omega) G_{iA}(\omega) \text{ and } \tilde{u}_{iB}(\omega) = \tilde{w}(\omega) G_{iB}(\omega), \quad (17)$$

similar to those from equations 5. Changing integration in equation 14 to summation and simplifying the integrand in the same manner as in equation 16, we have

$$V\tilde{S}_{AB} = \sum_{i=1}^I W_i \tilde{u}_{iA}^*(\omega) \tilde{u}_{iB}(\omega) = |\tilde{w}(\omega)|^2 \sum_{i=1}^I W_i G_{iA}^*(\omega) G_{iB}(\omega), \quad (18)$$

where the Green's functions are the results of measurements. The virtual source waveforms  $VS(t)$  thus have zero-phase spectra  $|\tilde{w}(\omega)|^2$ . Note that this computation does not require knowledge of medium velocity. Assuming  $W_i = 1$  in equation 18 and after reverting to the time domain, we obtain

$$VS_{AB}(t) = \sum_{i=1}^I u_{iA}(-t) * u_{iB}(t), \quad (19)$$

where  $*$  denotes convolution. Equation 19 is analogous to equation 1 in Bakulin and Calvert (2004) and is the crosscorrelation of traces  $u_{iA}(t)$  and  $u_{iB}(t)$ . Therefore, VSM can be deduced directly from the KHI. The traveltimes-based explanations of VSM (Schuster, 2005) apply only to simple models, while the considerations above indicate that medium complexity is not a restricting factor. Since the function  $\tau_G$  is taken directly from recorded data, it requires no interpretation in terms of separate wave arrivals and can be the product of complex multiarrival interference.

The obtained results can be explained in terms of time reversal. Indeed, to simulate the field recorded at the real source points  $D_i$ , ( $i = 1, 2, \dots, I$ ) from the virtual source at  $A$ , we use reciprocity and reverse time in the data set  $\tilde{u}_{iA}(\omega)$ . This allows the data from all the sources to be transformed to the same origin time at the point  $A$ , describing a back-propagation process in reverse time. In practice, however, because of the partial source coverage on  $\Sigma$  and the simplified integrand in equation 18, the radiation pattern of the

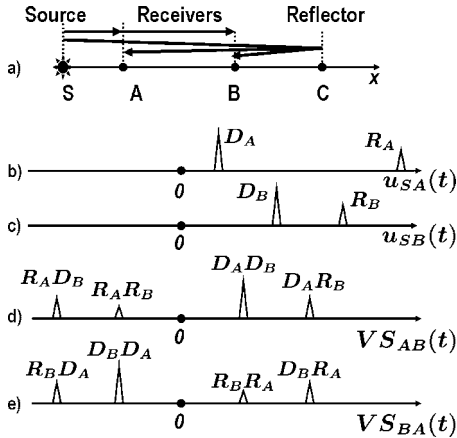


Figure 3. An explanation of the information content of causal and acausal responses obtained with approximate equation 19 and limited apertures: (a) 1D model with source  $S$  on the left, two receivers at  $A$  and  $B$ , and reflector at depth  $C$ ; (b) impulse seismogram at point  $A$  with direct  $D_A$  and reflected  $R_A$  waves; (c) similar response at point  $B$ ; (d) response  $VS_{AB}(t) = u_{SA}(-t) * u_{SB}(t)$  at  $B$  when the virtual source is at  $A$ . Note that  $D_A D_B$  (direct wave from  $A$  to  $B$ ) and  $D_A R_B$  (reflection from  $A$  to  $B$ ) map into the causal part ( $t > 0$ ) because both  $D_B$  and  $R_B$  arrive later than  $D_A$ . Analogously, waves  $R_A R_B$  (direct wave from  $B$  to  $A$ ) and  $R_A D_B$  (reflection from  $B$  to  $A$ ) appear in the acausal part ( $t < 0$ ) since events  $R_B$  and  $D_B$  both arrive earlier than  $R_A$ ; (e) response  $VS_{BA}(t) = u_{SB}(-t) * u_{SA}(t)$  at  $A$  when virtual source is at  $B$ . Analogous considerations demonstrate that the acausal part of  $VS_{AB}(t)$  moves into the causal part of  $VS_{BA}(t)$  and vice versa, as predicted by equation 20. Note that while arrival times on virtual source traces are symmetric ( $t_{D_A D_B} = t_{R_A R_B}, t_{D_A R_B} = t_{R_A D_B}$  or  $t_{R_B R_A} = t_{D_B D_A}, t_{D_B R_A} = t_{R_B D_A}$ ) with respect to  $t = 0$ , the amplitudes are not because of the incomplete aperture. For a complete aperture (additional source to the right of reflector  $C$ ), virtual source traces (d) and (e) would be purely symmetric and identical to each other.

virtual source will depend on the acquisition geometry, data complexity, and choice of weighting coefficients  $W_i$ .

Note that while for limited apertures equation 14 is not true, the functions of form 18 also consist of causal and acausal parts. While the causal parts represent waves propagating from point  $A$  to point  $B$ , for the acausal parts the direction of propagation is reversed as it follows equation 18, and

$$\widetilde{VS}_{AB}(\omega) = \widetilde{VS}_{BA}^*(\omega), \quad VS_{AB}(t) = VS_{BA}(-t). \quad (20)$$

If the virtual source data are computed at each receiver, then just the causal parts of the records have to be considered and any addition of acausal parts brings no extra information. Figure 3 illustrates this point for a simple 1D model.

## CONCLUSIONS

VSM can be regarded as an application of a modified Kirchhoff-Helmholtz integral to time-reversed data recorded in the subsurface using a distant array of sources either at the surface or in a borehole. We have demonstrated that VSM can accurately redatum

input data to downhole receiver locations below a shallow heterogeneous overburden. After such redatuming, the reflections from deep target horizons have higher signal-to-noise ratio because they are not distorted by the complex medium above. That should improve the quality of subsequent data migration. Our derivation involves no restrictions on medium complexity; therefore, VSM can be used for arbitrarily heterogeneous anisotropic elastic media and various acquisition geometries. Numerous conditions strictly needed to apply the KHI are not satisfied in practice, so it is unlikely that VSM can reconstruct true amplitudes of Green's functions between subsurface points. Still, considerations above provide reasonable assurance that VSM can accurately recover phase responses needed for high-fidelity imaging. In the presence of a full aperture (never attainable in practice), the theoretical response is antisymmetric in time. In approximate implementation with crosscorrelations and limited apertures, the acausal and causal parts are generally different. However, when the virtual sources are created at all receivers, the information contained in causal parts and acausal parts is redundant. The actual performance of VSM in realistic situations is the subject of the next investigation, which will be expanded to elastic models and three-component data.

## ACKNOWLEDGMENTS

This work was done at the Center for Computational Seismology (CCS) and has been supported by the U.S. Dept. of Energy under contract DE-AC03-76SF00098 and Shell International E&P. We thank Joe Dellinger and an anonymous reviewer for useful suggestions. We are especially grateful to the third reviewer, Ken Larner, for challenging and valuable help.

## REFERENCES

- Alexeev, A. S., and B. Y. Gelchinsky, 1958, About ray method for wavefields formed in inhomogeneous media with curved interfaces: *Voprosy Dinamicheskoi Teorii Rasprostraneniya Seismicheskikh*, 3, Nauka (in Russian).
- Baker, B. B., and E. T. Copson, 1950, *The mathematical theory of Huygens' principle*, 2nd ed.: Oxford University Press.
- Bakulin, A., and R. Calvert, 2004, Virtual source: New method for imaging and 4D below complex overburden: 74th Annual International Meeting, SEG, Expanded Abstracts, 2477–2480.
- , 2006, The virtual source method: Theory and case study: *Geophysics* (in print).
- Fink, M., and C. Prada, 2001, Acoustic time-reversal mirrors: *Inverse Problems*, 17, R1–R38.
- Morse, P. M., and H. Feshbach, 1953, *Methods of theoretical physics*: McGraw-Hill Book Company.
- Petrashen, G. I., and S. A. Nakhmkin, 1973, Continuation of wave fields in exploration seismology (*Prodolzhenie volnovykh polei v zadachakh seismorazvedki*): Nauka (in Russian).
- Schuster, G. T., 2005, Fermat's interferometric principle for target-oriented traveltome tomography: *Geophysics*, 70, U47.
- Timoshin, Y. V., 1978, *Impulse seismic holography*: Nedra (in Russian).
- van Manen, D.-J., J. O. A. Robertsson, and A. Curtis, 2005, Modeling of wave propagation in inhomogeneous media: *Physics Review Letters*, 94, 164301.
- Vasil'yev, S. A., 1975, On the possibility of continuing a seismic field into a stratified homogeneous medium: *Izvestiya, Academy of Sciences, USSR, Physics of the Solid Earth*, 9, 574–580.
- Wapenaar, K., 2004, Retrieving the elastodynamic Green's function of an arbitrary inhomogeneous medium by cross correlation: *Physics Review Letters*, 93, 254301.